A Snake Model for Anatomic M-mode Tracking in Echocardiography

N. Malpica, A. Santos
Dpto. Ingeniería Electrónica, Universidad Politécnica de Madrid
nmalpica,andres@die.upm.es
E. Pérez, M. García-Fernández
Laboratory of Echocardiography, Department of Cardiology
Hospital General Universitario Gregorio Marañón
M. Desco
Medicina y Cirugía Experimental, Hospital G. Universitario Gregorio Marañón
desco@mce.hggm.es

Abstract

The use of Tissue Doppler Imaging Imaging (TDI) has allowed to obtain velocity, strain and strain rate parameters in real time and is currently used routinely in the echocardiography lab. For analysis2D image sequences, profiles are marked on the image, and quantitative time profiles are obtained from them, a procedure known as anatomic M-mode. For correct quantification, the position of the region of interest must be tracked along the sequence. We propose a model for tracking profiles using a dual grey level/ TDI acquisition. Curves are tracked on the grey level sequence using an optical flow-based snake model and accurate TDI values are obtained from the tracked curve.

1. Introduction

Tissue Doppler imaging (TDI) is a relatively recent non-invasive ultrasound technique that allows the measurement of velocities at any point in the ventricular wall during the cardiac cycle. It produces velocity maps, displayed as a colour overlay superimposed on the grey-scale 2-D or M-mode image [1, 2] [3]. M-mode or 2-D tissue Doppler images also allow for the analysis of regional left ventricular wall motion dynamics [4]. The ability of TDI to provide information on the exact timing and magnitude of intramural wall velocities makes it a promising tool for the diagnosis of myocardial ischaemia. M-mode TDI has been widely studied for this purpose [5] [6]. Gradients between velocity values in different myocardial layers, computed using M-mode TDI images have also been shown to provide diagnostic information [7]. 2D TDI provides information on the complete myocardium. The use of 2D images allows to compute strain and strain rate images, which show the degree and rate of deformation of a tissue segment along the heart cycle [8].

On 2D images, velocity profiles and their evolution along time can be obtained from any line of the heart wall selected by the user, a procedure usually known as anatomic M-mode [9]. The user manually selects a certain line in the first image of the sequence. As the heart moves within the ultrasonic image during the cardiac cycle, tracking of the region is important to make sure that the extracted velocity traces represent the same myocardial segment over the whole cardiac cycle. In current applications the trace is moved either manually or automatically, by maintaining it in the middle of the heart wall along the sequence [10]. More accurate tracking of the curve is not possible using only the TDI information, as regional values change from one frame to the next.

Speckle tracking using optical flow techniques on standard ultrasound images has been widely studied and applied. An evaluation of differential methods on synthetic ultrasound images was reported in [11]. Optimization of block-matching methods for speckle was carried out in [12]. Speckle tracking has been used to obtain the velocity field of the heart [13] as well as to guide segmentation algorithms in image sequences [14, 15].

In this work we propose an accurate tracking procedure for anatomic M-mode curves based on the simultaneous acquisition of grey and TDI information. The grey level sequence is used to track the curve using a snake model driven by optical flow estimates. The anatomic M-mode is then automatically obtained from the corresponding TDI sequence.

Moreau and Cohen [16] combined grey level and TDI information to estimate the deformation field in every point of the heart, using the TDI information as a regularity constraint in the optical flow calculation. In our case, we only need to track a profile, thus not needing to compute a dense displacement field.

The paper is organized in the following way: The next section describes image acquisition. In section 3 the snake model is described with the motion estimation method used. Results are presented in section 4, followed by a discussion in section 5.

2. Image acquisition

Images were acquired with a 3 Mhz transducer using a Sequoia© scanner (Siemens-Acuson) with dual acquisition mode. A two-chamber view was obtained, centering the septum in the image. Grey scale images were acquired simultaneously. Sequences were acquired at 42 frames/sec. Figure 1 shows a grey-scale image of the septum and its corresponding TDI image.

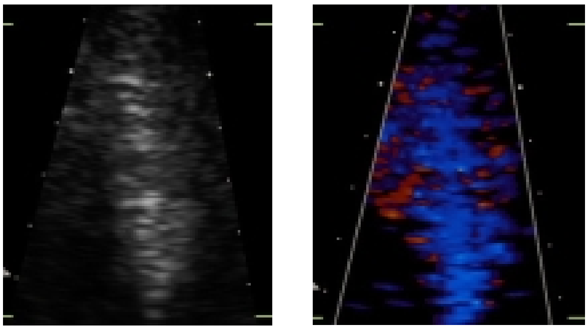

Figure 1. Grey level frame and corresponding TDI frame

To analyze the sequence, a profile is selected by the user in the first frame an a representation of the velocity profile along time is obtained. There is a need to track the position of the profile along time.

3. Snake model

The main title (on the first page) should begin 1-3/8 inches (3.49 cm) from the top edge of the page, centered, and in Times 14-point, boldface type. Capitalize the first letter of nouns, pronouns, verbs, adjectives, and adverbs; do not capitalize articles, coordinate conjunctions, or prepositions (unless the title begins with such a word). Leave two blank lines after the title.

A special attention has been devoted in the past years to image segmentation using snakes. Snakes were first introduced by Kass et al. [17] as a means to combine low-level processing with higher level knowledge. They proposed energy minimization as a framework where low-level information, usually image gradient or image intensity can be combined with higher level information (usually shape, continuity of the contour or user interactivity). The energy of the snakes is usually expressed in terms of external constraint forces such as lines, edges and region homogeneities found in the image, and of internal forces which impose smoothness constraints on the modeled contours. Snakes have been widely used to track contours in image sequences. In the original work by Kass et al. the tracking was performed using as initial position in the current frame the final position reached in the preceding frame. Blake [18] and Peterfreund [19] solved the tracking problem using Kalman filtering estimation. Giachetti [14] estimated the initial snake on a frame by displacing the result of the preceding frame using optical flow. Mikic [15] integrated the optical flow estimation into the minimization process. Recently, Pardas [20] used the optical flow estimation to restrict the candidates for the minimization process. In all of these cases, the snake was driven mainly by edge information. In our case, the aim is the tracking of a curve drawn inside the myocardium so no edge information is available. The only external force of the snake is the optical flow estimation.

In the discrete formulation of active contours, the contour is represented as a set of vertices (known as snaxels) vi = (xi,yi) for i = 0,…,N-1, where xi and yi are the x and y coordinates of snaxel i, and its energy, which is going to be minimized is defined by:

$$E_{snake} = \sum_{i=0}^{N-1} \left(E_{\mathrm{int}}(v_i) + E_{ext}(v_i) \right)$$

In our model, the snake has two energies, an internal energy based on curvature and an energy based on the estimation of image motion.

The complete model based on curvature and motion energies is:

$$E_{tot} = \alpha E_{curv} + \beta E_{mot}$$

where α and β are parameters controlling the contribution of the different energies in every point. Parameters can be different in every point depending, for instance on the quality of the correlation at that point. In this work both parameters were constant in space and in time.

3.1. Internal Energy

The internal energy, Eint, is normally based on the discrete first or second derivatives, to ensure that the contours remains smooth and tend to be round. We use the concept of curvature, defined as in [21] (see Fig. 2).

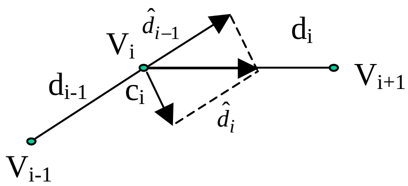

Figure 2. Details of snake vertices showing the local curvature vector.

The snake model is composed of vertices vi. The edge between vi and vi+1 is denoted by d_i. The direction of the edge is described by the unit vector $\hat{d}_i$. The local curvature at the position of a vertex is defined as the difference between the directions of the two edge vectors that join at that location:

$$c_i = \hat{d}_i - \hat{d}_{i-1}$$

As can be seen, the curvature is zero when both lines ending at a vertex are parallel. Minimization of curvature would lead to a straight snake. In our application, the user draws the initial profile in the myocardium, and we wish to maintain the shape of that curve. The internal energy in our model is therefore designed to maintain the initial local curvature. The local curvature is computed at every point of the initial profile. At every iteration, the local curvature is computed at every candidate point and the curvature energy is obtained as the difference with the initial curvature at that snaxel. We are using an open snake model, so special care should be taken for processing the extrema. The curvature at the first and last point of the snake is defined as the direction of the first and last segments, respectively.

3.2 External energy: Optical flow

To track the snake along the sequence, the external energy is based on the estimation of interframe motion. Methods for computing displacement between two frames in a sequence are generally classified into two groups: Block matching methods and differential methods [22]. The first ones try to minimize a certain distance between pixels in a neighborhood around the point, generally the square difference, or to maximize a correlation measure [14]. The second ones are based on temporal and spatial gradient computations. We use a scheme of the first type, proposed recently by Cohen et al. [23] for ultrasound images.

Let Xt be a set of coordinates of an image at time t. Let $I_t(x_t)$ represent the intensity of a pixel at the coordinates x_t and let $I_t=\{I_t(x_t)\}$, $x_t \in X_t$, represent the intensity image at time t. The transition of a pixel between t-1 and t is described by the motion vector $v_i(x_t)$. If $x_{t-1} \in X_{t-1}$ is the pixel corresponding to $x_t \in X_t$, the following stands:

$$v_t(x_i) = x_t - x_{t-1}$$

According to the maximum likelihood method for parameter estimation, the ML estimate of v_t, $\hat{v}_{ML}$ is obtained by maximization of the conditional probability density

$$\max_{v_t} p(I_{t-1}/I_t, v_i) \ at \ v_t = \hat{v}_{ML}$$

If Ai is a region with constant motion around a certain point. Let $a_i = [a_{i1}...a_{ik}]^T$ represent the vector for all intensities $I_{t-1}(x_{t-1})$, $x_{t-1} \in A_i$ and $b_i = [b_{i1}...b_{ik}]^T$ the corresponding vector of intensities $I_t(x_t)$, where $x_t = x_{t-1} + v_i$. The maximization of equation (2) is equivalent to the maximization for each i of the following conditional probability density functions:

$$\max_{v_t} p(a_i/b_i, v_i) \ at \ v_t = \hat{v}_{ML}$$

Making the assumption of multiplicative Rayleigh noise, when the noiseless value at pixel i is s_i the observed pixels in both frames are $a_i = n_{i1}s_i$ and $b = n_{i2}s_i$ where n_{i1} and n_{i2} are two independent noise elements with Rayleigh density functions. The relation between noisy pixels in both frames then becomes:

$$a_i = \eta_i b_i \qquad \text{where } \eta_i = n_{i1} / n_{i2}$$

Taking into account that the noise term ηi is the division of two Rayleigh distributed random variables, the conditional probability density function [23] is given by

$$p(a_i/b_i, v_i) = \prod_{j=1}^{k} \left\{ \frac{2(a_i/b_i)^2}{\left[(a_i/b_i)^2+1\right]^2} \right\}$$

For a specific vertex, the corresponding point in the next frame is computed by maximum likelihood. At every point in the search area, the correlation energy E_{mot} is equal to the distance to that point, so a minimum is obtained exactly in the desired location.

3.3 Minimization

In the original work, Kass et al. [17], searched for a global minimum using variational calculus. More efficient approaches using dynamic programming have also been proposed. We use the 'greedy' algorithm proposed by Williams and Shah [24]. During each iteration, a neighborhood of each point is examined and the point in the neighborhood giving the smallest value for the energy term is chosen as the new location of the point. Although the algorithm is not guaranteed to reach a global minimum, it is much faster than other methods, yielding comparable results.

4. Results and Discussion

The model was tested on 10 sequences. A search region of 5x5 pixels and a correlation window of 15x15 were used in all experiments. An expert user was asked to draw a profile on the first image and the curve was automatically tracked throughout the whole sequence. Results of curve tracking on gray and on TDI sequences are shown in figures 3 and 4. These results were obtained with $\alpha = 0.8$, $\beta = 1.0$. For the first sequence, grey level data is presented. The second result is presented with the profile superimposed on the TDI sequence.

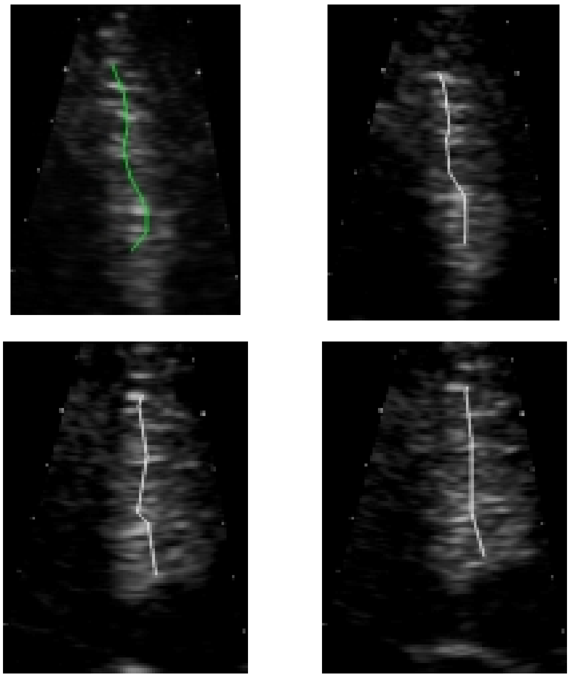

Figure 3. Frames of a gray level sequence showing the automatic tracking of the curve

An anatomic M-mode is then obtained from the tracked curve. Figure 5 shows the resulting M-modes obtained from the curves tracked in the sequences of figures 3 and 4.

As can be seen, the size of the curve changes due to heart motion, so the resulting anatomical M-mode has a changing number of columns, as compared to the result of simply maintaining the fixed curve in the centre of the myocardium.

We have developed a platform for echocardiographic quantification which is used for research in our center. Anatomic M-mode tracking is currently performed by manually repositioning the curve, and no tracking method has yet been presented for this purpose [25]. On all of the sequences tested with our method, the automatic repositioning result was considered good enough from the point of view of the clinical user.

Only a visual evaluation by clinical users has been performed. In current clinical practice, the user adjusts the profile on TDI images by assuring that the line stays within the myocardial wall. No tracking is manually done on the grey level sequence, so a direct comparison of our method and user defined positions is not feasible.

A limitation of the method is the fact that we can only capture in-plane motion. Due to plane shifts, the speckle pattern is not constant along time. inherent to all quantification methods using 2D echocardiography. This, however, is a problem inherent to all 2D echocardiography processing methods, that will be solved when 3D echocardiography becomes feasible to be used in clinical routine.

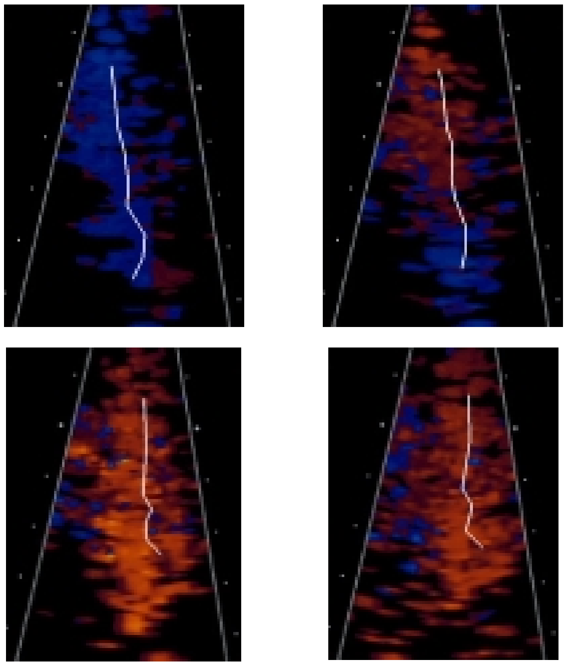

Figure 4. Frames of TDI level sequence showing the automatic tracking of the curve

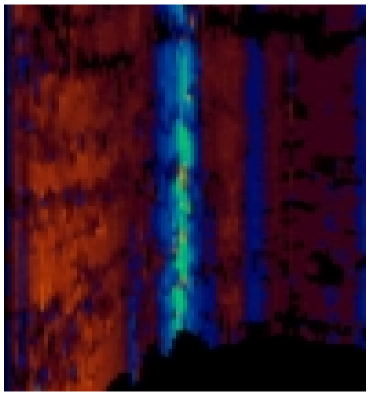

Figure 5. Anatomic M-mode image obtained from a 2D sequence.

5. Conclusion

We have proposed a model for curve tracking in the myocardium, which allows to obtain accurate anatomic M-representations images from 2D TDI images. The continuity constraint was designed to maintain the initial shape of the curve selected by the user. Other forces could be directly introduced in the model to smooth the curve. We have analyzed images of the septum but the model can be used to track any curve in quantitative studies. Future research is oriented at measuring the quality of the correlation an using this factor to control the iteration process.

6. References

[1] M. Desco and J. C. Antoranz, "Technical principles of Doppler Tissue Imaging," in *Doppler Tissue Imaging*, M. A. García-Fernández, J. L. Zamorano, and J. Azevedo, Eds. New York: McGraw-Hill, 1997.

[2] P. Palka, A. Lange, A. D. Fleming, G. R. Sutherland, L. N. Fenn, and W. N. McDicken, "Doppler tissue imaging: Myocardial wall motion velocities in normal subjects," *J Am Soc Echocardiogr*, vol. 8, pp. 659-68, 1995.

[3] G. R. Sutherland, B. Bijnens, and W. N. McDicken, "Tissue Doppler Echocardiography: Historical Perspective and Technological Considerations," *Echocardiography*, vol. 16, pp. 445-453., 1999.

[4] M. A. García-Fernández, J. L. Zamorano, and J. Azevedo, *Doppler Tissue Imaging*. New York: McGraw-Hill, 1997.

[5] G. Derumeaux, M. Ovize, J. Loufoua, X. Andre-Fouet, Y. Minaire, A. Cribier, and B. Letac, "Doppler tissue imaging quantitates regional wall motion during myocardial ischemia and reperfusion," *Circulation*, vol. 97, pp. 1970-7, 1998.

[6] M. Desco, M. J. Ledesma-Carbayo, E. Pérez, A. Santos, J. C. Antoranz, N. Malpica, M.-A. P., and M. A. García-Fernández, "Assessment of Normal and Ischaemic Myocardium by Quantitative M-mode Tissue Doppler Imaging," *Ultrasound in Medicine and Biology*, vol. 18, pp. 561-569, 2002.

[7] P. Marcos-Alberca, M. A. Garcia-Fernandez, M. J. Ledesma, N. Malpica, A. Santos, M. Moreno, J. Bermejo, J. C. Antoranz, and M. Desco, "Intramyocardial analysis of regional systolic and diastolic function in ischemic heart disease with Doppler tissue imaging: role of the different myocardial layers," *J Am Soc Echocardiogr*, vol. 15, pp. 99-108, 2002.

[8] A. Heimdal, A. Stoylen, H. Torp, and T. Skjaerpe, "Real-time strain rate imaging of the left ventricle by ultrasound," *J Am Soc Echocardiogr*, vol. 11, pp. 1013-9, 1998.

[9] D. Mele, I. Pedini, P. Alboni, and R. A. Levine, "Anatomic M-mode: a new technique for quantitative assessment of left ventricular size and function," *Am J Cardiol*, vol. 81, pp. 82G-85G, 1998.

[10] G. R. Sutherland, T. Kukulski, J. U. Voight, and J. D'Hooge, "Tissue Doppler Echocardiography: Future Developments," *Echocardiography*, vol. 16, pp. 509-520, 1999.

[11] P. Baraldi, A. Sarti, C. Lamberti, A. Prandini, and F. Sgallari, "Evaluation of differential optical flow techniques on synthesized echo images," *IEEE Transactions on Biomedical Engineering*, vol. 43, pp. 259-272, 1996.

[12] F. Yeung, S. F. Levinson, and K. J. Parker, "Multilevel and Motion Model-Based Ultrasonic Speckle Tracking Algorithms," *Ultrasound in medicine and biology*, vol. 24, pp. 427-441, 1998.

[13] G. E. Mailloux, F. Langlois, P. Y. Simard, and M. Bertrand, "Restoration of the velocity field of the heart from two dimensional echocardiograms," *IEEE Transactions on Medical Imaging*, vol. 8, pp. 143-153, 1989.

[14] A. Giachetti, "On-line analysis of echocardiographic image sequences," *Medical Image Analysis*, vol. 2, pp. 261-284, 1998.

[15] I. Mikic, S. Krucinski, and J. D. Thomas, "Segmentation and tracking in echocardiographic sequences: active contours guided by optical flow estimates," *IEEE Trans Med Imaging*, vol. 17, pp. 274-84, 1998.

[16] V. Moreau, L. Cohen, and D. Pellerin, "Deformation Field Estimation for the Cardiac Wall using Doppler Tissue Imaging," presented at *Functional Imaging and Modeling of the Heart, First International Workshop*, Helsinki, Finland, 2001.

[17] M. Kass, A. Witkin, and D. Terzopoulos, "Snakes: Active contour models," *International Journal of Computer Vision*, vol. 1, pp. 321-331, 1988.

[18] A. Blake, R. Curwen, and A. Zisserman, "A framework for spatiotemporal control in the tracking of visual contours," *International Journal of Computer Vision*, vol. 11, pp. 127-145, 1993.

[19] N. Peterfreund, "Robust Tracking of Position and Velocity With Kalman Snakes," *IEEE Transactions on Pattern Analysis and Machine Intelligence*, vol. 21, pp. 564-569.

[20] M. Pardas and E. Sayrol, "Motion estimation based tracking of active contours," *Pattern Recognition Letters*, vol. 22, pp. 1447-1456, 2001.

[21] S. Lobregt and M. A. Viergever, "A discrete dynamic contour model," *IEEE Transactions on Medical Imaging*, vol. 14, pp. 12-24, 1995.

[22] J. L. Barron, D. J. Fleet, and S. S. Beauchemin, "Performance of optical flow techniques," *International Journal of Computer Vision*, vol. 12, pp. 43-77, 1994.

[23] B. Cohen and I. Dinstein, "New maximum likelihood motion schemes for noisy ultrasound images," *Pattern Recognition*, vol. 35, pp. 455-463, 2002.

[24] D. J. Williams and M. Shah, "A Fast Algorithm for Active Contours and Curvature Estimation," *CVGIP: Image Understanding*, vol. 55, pp. 14-26, 1992.

[25] J. D'hooge, B. Bijnens, J. Thoen, F. Van de Werf, G. R. Sutherland, and P. Suetens, "Echocardiographic strain and strain-rate imaging: a new tool to study regional myocardial function," *IEEE Trans Med Imaging*, vol. 21, pp. 1022-1030, 2002.